The Plant Cell, Vol. 16, 3059–3068, November 2004, www.plantcell.org

Optimization and Evolution of Light Harvesting in Photosynthesis: The Role of Antenna Chlorophyll Conserved between Photosystem II and Photosystem I

Sergej Vasil'ev[1] and Doug Bruce

Department of Biological Sciences, Brock University, St. Catharines, Ontario, L2S 3A1, Canada

The efficiency of oxygenic photosynthesis depends on the presence of core antenna chlorophyll closely associated with the photochemical reaction centers of both photosystem II (PSII) and photosystem I (PSI). Although the number and overall arrangement of these chlorophylls in PSII and PSI differ, structural comparison reveals a cluster of 26 conserved chlorophylls in nearly identical positions and orientations. To explore the role of these conserved chlorophylls within PSII and PSI we studied the influence of their orientation on the efficiency of photochemistry in computer simulations. We found that the native orientations of the conserved chlorophylls were not optimal for light harvesting in either photosystem. However, PSII and PSI each contain two highly orientationally optimized antenna chlorophylls, located close to their respective reaction centers, in positions unique to each photosystem. In both photosystems the orientation of these optimized bridging chlorophylls had a much larger impact on photochemical efficiency than the orientation of any of the conserved chlorophylls. The differential optimization of antenna chlorophyll is discussed in the context of competing selection pressures for the evolution of light harvesting in photosynthesis.

INTRODUCTION

In photosynthetic systems a variable number of pigments act as light-harvesting antenna to absorb and direct solar energy to photochemical reaction centers (RC). The effectiveness of the RC depends on the efficient transfer of excitation energy from these antenna molecules.

All known RCs share a similar structural blueprint: two sets of five transmembrane helices holding six porphyrin and two quinone cofactors arranged in two membrane-spanning branches (Michel and Deisenhofer, 1988; Nitschke and Rutherford, 1991; Blankenship, 1992; Barber and Andersson, 1994; Rhee et al., 1998; Schubert et al., 1998). RCs differ in the number and position of antenna porphyrins (core antenna) associated with this basic structural unit, and in their differential association with a variety of auxiliary protein complexes.

RCs where electron transport terminates at iron sulfur centers are classified as Type I, and RCs whose terminal electron acceptors are quinones are Type II (Blankenship, 1992). Type I RCs are found in anaerobic green sulfur bacteria, heliobacteria, and in oxygenic photosynthetic organisms as the photosystem I (PSI) complex. Type I RCs have two main homologous structural polypeptides, denoted as PsaA and PsaB in case of PSI. Each of these polypeptides can be divided into regions based on function (Krauß et al., 1996; Schubert et al., 1998; Klukas et al., 1999). The first five membrane-spanning helices, at the C-terminal end, associate together to form the RC domain that holds the electron-transfer cofactors. The N-terminal region of each of the Type I polypeptides has six membrane-spanning helices that bind the core antenna light-harvesting (bacterio)chlorophylls and carotenoids.

Type II RCs are found in purple bacteria, green filamentous bacteria, and in the photosystem II (PSII) complex of oxygenic photosynthetic organisms. The Type II RC polypeptides responsible for holding the electron transport cofactors (denoted D1/D2 in PSII) are smaller than their counterparts in Type I RCs but have a strong homology with the first five membrane spanning helixes at the C-terminal end of the Type I RC polypeptides (Krauß et al., 1996; Rhee et al., 1998; Schubert et al., 1998; Klukas et al., 1999; Ben Shem et al., 2003). In contrast with Type I centers the Type II RCs noncovalently interact with separate membrane-bound core antenna pigment binding proteins such as CP47 and CP43 in the case of PSII. Interestingly, these six-helix antenna proteins of PSII have strong structural homologies with the core antenna domains (the six transmembrane helixes at the N-terminal end) of the PSI polypeptides (Rhee et al., 1998; Schubert et al., 1998).

The number of core antenna pigments is variable between different types of reaction centers. In oxygenic organisms the PSII core antenna consists of ~40 chlorophylls whereas the PSI core antenna consists of ~100 chlorophylls. The protein folding of the antenna systems in nonoxygenic organisms with Type I reaction centers (green sulfur bacteria, heliobacteria) is similar to

[1] To whom correspondence should be addressed. E-mail svassili@brocku.ca; fax 905-688-1855.

The author responsible for distribution of materials integral to the findings presented in this article in accordance with the policy described in the Instructions for Authors (www.plantcell.org) is: Sergei Vasil'ev (svassili@brocku.ca.).

Article, publication date, and citation information can be found at www.plantcell.org/cgi/doi/10.1105/tpc.104.024174.

PSI, but the number of core antenna pigments associated with each reaction center is smaller. Nonoxygenic Type II reaction centers, found in purple bacteria, do not have pigment-protein complexes analogous to the core antenna parts of PSII. Instead, these reaction centers are surrounded by an oligomeric ring of small pigment binding polypeptides (LH-1).

High-resolution atomic structures have been determined for PSI (Jordan et al., 2001) and PSII complexes (Ferreira et al., 2004) from cyanobacteria. These detailed structures of photosystems from oxygenic organisms have provided an opportunity for better understanding the light-harvesting function by computational examination of the excitation pathway from absorption of photon to primary electron transfer in the RC (Byrdin et al., 2002; Damjanovic et al., 2002; Vasil'ev et al., 2001, 2002). In a previous computational study of PSI, the orientations of all antenna chlorophylls were sampled randomly and the quantum yields of kinetic models based on the randomized structures calculated (Sener et al., 2002). Interestingly, the native structure had a higher quantum yield than the majority of random structures suggesting the antenna chlorophyll orientations had been optimized for energy transfer over the course of evolution. In a similar computational study of excited-state dynamics in PSII we found the quantum yield of the native structure of antenna chlorophylls to be no higher than the average yield of the randomly oriented models (Vasil'ev et al., 2004). Our study of PSII did, however, reveal large differences in the optimization of different groups of antenna chlorophylls. A group of six bridging antenna chlorophylls, located close to the RC, were found to be highly optimized. Because these bridging chlorophylls carry much of the excitation energy from the antenna to the RC, their orientations may be expected to reflect selection pressure for optimizing quantum yield. By contrast, the orientations of two peripheral chlorophylls ($Chl_{Z/D}$) in the PSII RC domain were very unfavorable for excitation transfer from the antenna to the RC (Vasil'ev et al., 2004). These two $Chl_{Z/D}$ can function as electron donors to $P680^+$ (Depaula et al., 1985; Faller et al., 2000) and, thus, serve roles in addition to light harvesting. Interestingly, the His residues homologous to the axial ligands of $Chl_{Z/D}$ are conserved in PSI and in all Type I RC sequences believed to be ancestral to PSI and PSII (Baymann et al., 2001). The orientations of $Chl_{Z/D}$ may, thus, also be influenced by evolutionary constraint(s) related to assembly, structural stability, or interaction with other components of the photosynthetic apparatus.

It is not known whether the PSI antenna structure has a similar motif to that found in PSII, where the orientations of some pigments are highly optimized for energy transfer and others are not. This question is particularly interesting because several residues that provide the fifth ligand to the Mg atom of the (bacterio)chlorophyll antenna molecules have been previously shown to be conserved over the course of evolution among a large group of photosynthetic organisms including green sulfur bacteria, heliobacteria, PSI, and PSII (Fyfe et al., 2002). To further explore potential similarities in the core antenna of PSII and PSI, we compared their x-ray structures and identified 26 highly conserved antenna chlorophylls.

These conserved chlorophylls represent significant fractions of the core antenna systems. Why have the positions and orientations of these chlorophylls been conserved? Are the conserved positions critical to energy transfer efficiency or do they reflect selection pressures related to assembly and/or maintenance of stable protein structure?

To answer these questions we performed a detailed analysis of the optimality of the conserved chlorophyll arrangements. Our results show that the conserved antenna chlorophylls are not orientationally optimized to maximize quantum yield. By extending our analysis to each individual antenna chlorophyll in PSI and PSII we found that the native orientations of very few were actually optimized for quantum yield of photochemistry. Each photosystem did, however, contain a pair of highly optimized bridging chlorophylls responsible for carrying much of the excitation energy from the antenna to the RC.

RESULTS

Comparing PSII and PSI Antenna Structure

According to a previous sequence alignment (Fyfe et al., 2002) five chlorophyll-liganding His residues were conserved between PsaA of PSI and CP43 of PSII. We oriented the PSI (pdb 1JBO; Jordan et al., 2001) and PSII (pdb 1S5L; Ferreira et al., 2004) structures to overlap the six homologous helices of PsaA and CP43. Four of the chlorophylls liganded to these His in PsaA were in almost identical positions in CP43. The chlorophyll coordinated by the fifth conserved His, H313 in PsaA, did not have a structural equivalent in CP43. However, a chlorophyll coordinated by Y315 did. Four additional chlorophylls, not identified in the previous sequence alignment (Fyfe et al., 2002), were observed to have very similar positions and orientations in PSI and PSII. To compare antenna systems in more detail, we fit the PSII structure to the PSI reference structure using only the Mg atoms of all nine matching chlorophylls. The obtained fit had a surprisingly good quality (root mean square distance deviation was <1.6 Å). Not only the positions but also the orientations of the porphyrin planes of all nine chlorophylls were found to be nearly identical in PsaA and CP43. Our fitting procedure also revealed two more potentially conserved chlorophyll. Chlorophyll A23 in PSI is coordinated by hydrogen bonding via a water molecule to Q355 or N359 and is equivalent to chlorophyll 23 in CP43. And finally, the position of chlorophyll A6 in PSI was found to be similar between PSI and PSII; this chlorophyll has no obvious Mg ligand in either structure. Altogether we found 11 conserved chlorophyll between PsaA and CP43 (Table 1).

When CP47 and PsaB were superimposed using the same fitting procedure described above, 13 equivalent chlorophylls were found (Table 1). In the case of CP47, seven chlorophyll ligands were the same as found previously by sequence alignment (Fyfe et al., 2002) and our structural comparison revealed six additional conserved chlorophylls.

We also aligned the D1/D2 domain of PSII with the RC core domain of PSI using a similar fitting procedure based on the two $Chl_{Z/D}$ and their PSI equivalents (Baymann et al., 2001). The location and orientation of the two $Chl_{Z/D}$ and their PSI equivalents are highly conserved, although the $Chl_{Z/D}$ are ~3.5 Å closer to the center of the D1/D2 complex (defined as the center of gravity of P680) than their PSI equivalents.

Table 1. Chlorophylls Conserved between PSI and PSII, Their Ligands, and Differences between PSI and PSII Structures in Positions (ΔR, Å) and Orientations ($\Delta\theta$, °) of These Chlorophylls

	PsaA		CP43		PsaA-CP43 fit *T. elongatus*/ *T. vulcanus*		PsaB		CP47		PsaB-CP47 fit *T. elongatus*/ *T. vulcanus*	
Helix	Ligand	Chlorophyll	Ligand	Chlorophyll	ΔR	$\Delta\theta$	Ligand	Chlorophyll	Ligand	Chlorophyll	ΔR	$\Delta\theta$
	H56	1	*N39*	44	2.6/na	14.1/na	H28	1	H9	32	1.5/0.9	6/98
I	**H76**	**3**	**H53**	**15**	**1.9/2.5**	**5.1/0.5**	**H49**	**2**	**H23**	**25**	**1.7/2.4**	**7.9/20**
I	**H79**	**4**	**H56**	**13**	**0.6/0.6**	**9.6/10**	**H52**	**3**	**H26**	**24**	**1.0/0.6**	**11/90**
	Q115?	*6*	*?*	*12*	*4.3/4.3*	*132/146*	*H88*	*5*	*?*	*26*	*3.2/3.9*	*123/131*
II	H179	8	H132	21	1.8/2.6	12/121	H155	8	H114	37	1.2/1.6	40/54
III	H200	11	H164	19	1.1/1.1	33/37	H177	10	H142	34	1.9/1.8	19/26
III							**H192**	**11**	**H157**	**27**	**1.3/2.3**	**14/14**
IV	**H301**	**17**	**H237**	**16**	**1.3/2.2**	**9.4/71**	**H276**	**15**	**H202**	**29**	**0.4/1.2**	**12/22**
IV	*Y315/W*	*19*	*H251*	*11*	*1.3/1.8*	*15/1.0*	*Y290/W*	*16*	*H216*	*23*	*1.2/1.4*	*13/94*
IV							**H275**	**14**	**H201**	**33**	**2.1/5.3**	**17/168**
V	*Q355/W*	*23*	*?*	*22*	*1.9/4.7*	*5.7/153*	*H340*	*21*	*S241?*	*36*	*3.5/4.8*	*7.1/115*
VI	H397	27	H430	18	1.8/1.1	32/133	**H378**	**25**	**H455**	**28**	**2.2/1.9**	**32/22**
VI	**H411**	**28**	**H444**	**20**	**0.8/0.3**	**7.8/5.4**	**H392**	**26**	**H469**	**35**	**1.3/0.7**	**3.5/21**
RC	**H540**	**36**	**H118**	**9**	**3.7/3.6**	**28/19**	**H527**	**35**	**H117**	**10**	**3.7/3.5**	**25/30**

Chlorophylls, for which homology was found previously by sequence alignment are shown in bold; underlined are chlorophylls that are conserved between PSII, PSI, and reaction centers from the green sulphur bacteria *C. lumicola* and heliobacteria *H. mobilis*. Chlorophylls for which homology was found by structure comparison are shown in regular type style. Chlorophylls that do not have an axial ligand in these structures or have ligands different from His are shown in italics. PSII chlorophyll numbers are as in 1S5L.pdb. Data for ΔR and $\Delta\theta$ are given for both the *T. elongatus* and *T. vulcanus* structures.

The rigid body fits of all three PSII domains to PSI were performed separately. Alignment of the entire PSII x-ray structure with PSI resulted in a poor overlap because of the larger distance between the antenna and the RC domains in PSII compared with PSI and the slightly different relative orientations of antenna and core domains of the two photosystems.

The independent alignment of the antenna and the RC domains of PSII with PSI that resulted from our rigid-body fits is shown in Figure 1 and a summary of our structural comparison is presented in Table 1. A total of 26 chlorophylls (not including reaction center chromophores) have very close structural equivalents in PSII and PSI. Twenty-four of these conserved chlorophylls are organized in two layers, one toward the stromal surface and the other toward the lumenal surface. The remaining two chlorophylls interconnect the two layers. We used PSII structures from both *Thermosynechococcus elongatus* (Jordan et al., 2001; Ferreira et al., 2004; Vasil'ev et al., 2004) and *Thermosynechococcus vulcanus* (Kamiya and Shen, 2003; Vasil'ev et al., 2004) in our analysis, and results for both are included in Table 1. Although the overlap of conserved chlorophylls in PSII with their equivalents in PSI is high for both PSII structures, it is higher with the 3.5-Å structure from *T. elongatus*. In that structure the dipole transitions of most of the conserved chlorophyll are within 15° of their PSI equivalents!

Why are the positions and orientations of these 26 chlorophylls so highly conserved between PSII and PSI? One explanation is that the conserved arrangement is designed optimally for light harvesting and energy transfer to the RC. To address this hypothesis we compare the efficiency of the conserved antenna chlorophyll subsystems with randomly generated chlorophyll arrangements.

For both PSI and PSII we generated an ensemble of models with alternate arrangements of the transition dipoles by random independent orientation of the antenna chlorophylls. Only the orientations of the dipoles varied, their positions, and thus the distances between them, were unchanged. We then assessed the quantum yield of photochemistry (as the yield of reduced quinone electron acceptors) of kinetic models for excitation energy transfer based on each of the resulting structural configurations. See Methods for more details. The results of simulations are represented as histograms of the yield distribution (Figures 2, 3, and 6). The number of scores in each histogram bin is equal to the number of models with alternate chlorophyll arrangements for which the quantum yield falls within the range of the bin. The histograms show the influence of the changing structural configurations on the calculated quantum yield and allow for easy comparison to the quantum yield of the native configuration. The quantum yield of the native configuration, shown by an arrow, divides the histogram into regions representing structural configurations with higher and lower quantum yields. The probability of attaining a quantum yield higher than the native configuration by chance is the number of structural configurations that predict a higher quantum yield (area under the histogram to the right of the native configuration) divided by all structural configurations tested (area of entire histogram).

Efficiency of the Conserved PSI/PSII Light-Harvesting Chlorophyll Subsystems

To investigate the possible optimality of the conserved antenna chlorophylls we constructed model antenna systems for both PSII and PSI that contained only these antenna chlorophylls.

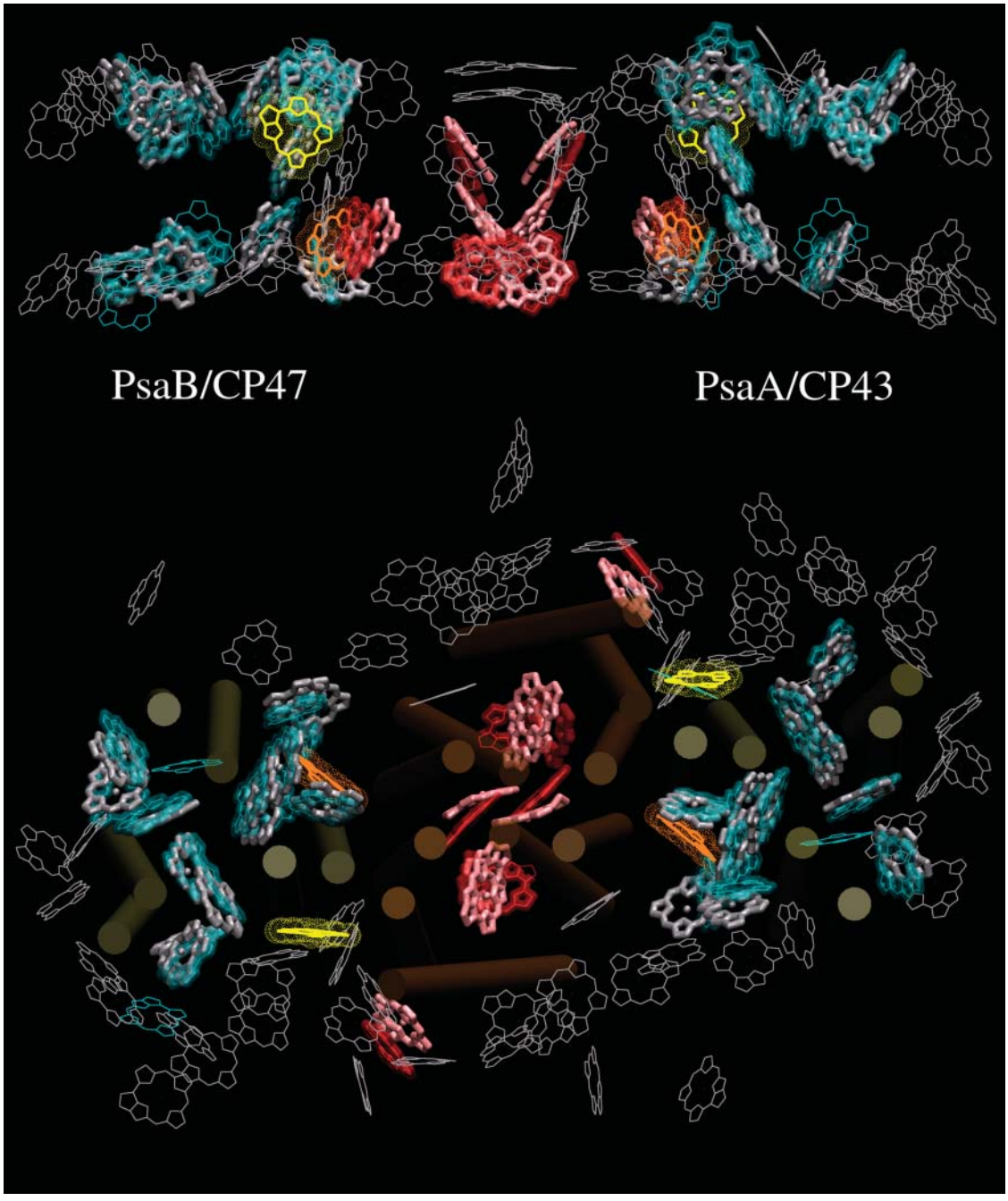

Figure 1. Comparison of PSI and PSII Structures.

The top panel is a side-on view from within the plane of the thylakoid membrane. The bottom panel is a view from the lumenal side. The individual domains of PSII (CP43, CP47, and D1/D2) are overlapped with the PSI structure as described in the text. Chlorophylls of the RC core domains of PSII (PSI) are shown in red (pink). Antenna chlorophylls of PSII (PSI) are shown in green (gray). Antenna chlorophylls that are conserved in both photosystems are shown with bold lines. Chlorophylls unique to one photosystem are shown with thin lines. The most important optimized connecting chlorophylls of PSII (PSI) are shown in yellow (orange).

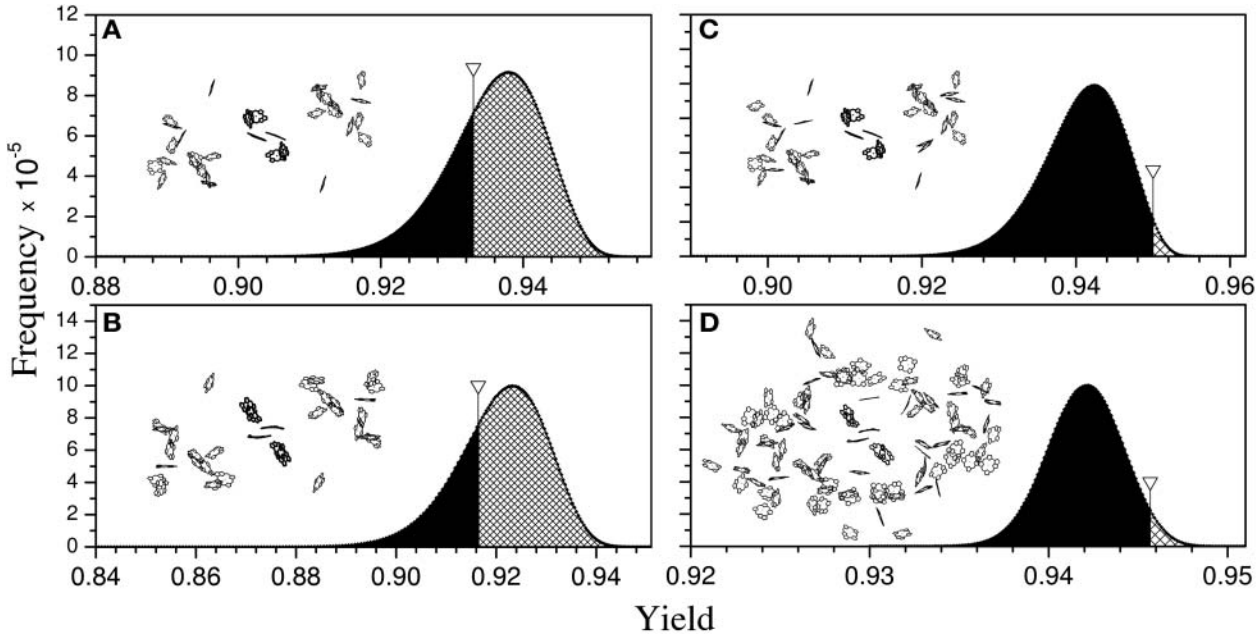

Figure 2. Histograms of the Quantum Yield Distributions Computed for Model Antenna Systems of PSII and PSI.

Inserts show the structure of the respective models. Arrows indicate the location of the quantum yield calculated with native chlorophyll orientations as found in the x-ray structures. Areas under the shadowed/black parts of the histograms represent the number of alternative pigment orientations with yields higher/lower than the native x-ray structure, respectively. Orientations of all antenna chlorophylls except $Chl_{Z/D}$ in the case of PSII and chlorophylls A39 and B40 in the case of PSI were varied.

(A) PSI including only the 26 chlorophylls conserved between PSI and PSII.

(B) PSII including 26 chlorophylls conserved between PSI and PSII.

(C) PSII including all antenna chlorophylls.

(D) PSI including all antenna chlorophylls.

In PSII, two of the conserved chlorophylls are the $Chl_{Z/D}$ molecules associated with the D1 and D2 reaction center proteins. These chlorophylls have been suggested to serve an alternative electron transport function in PSII, have previously been shown not to be oriented optimally for energy transfer (Depaula et al., 1985; Faller et al., 2000), and were thus fixed in their native orientation in our analysis. The directions of the dipoles of the remaining 24 conserved chlorophylls were varied in the model for PSII. As shown in Figure 2A most of the random orientations of this group of 24 conserved chlorophylls resulted in a higher quantum yield than the native configuration. The native orientations of the conserved chlorophyll are clearly not optimized for maximal quantum yield in PSII. The same result was found when the analogous model for PSI was analyzed (Figure 2B).

Interestingly, when the complete antenna system of PSII was considered, and the orientations of all antenna chlorophylls (except the two $Chl_{Z/D}$) were varied, the native configuration of the entire antenna was more optimized (Figure 2C) than that of the conserved subset (Figure 2A). The native orientation of the complete antenna system of PSI was also optimized more than the conserved subset, as shown in Figure 2D. The optimality of the entire PSI antenna has been observed previously (Sener et al., 2002).

Two additional models were designed to further test for optimality of the conserved antenna chlorophylls within the entire energy transfer networks of PSII and PSI. These models included all antenna chlorophylls, but only the orientations of the 24 conserved chlorophylls were varied and all other chlorophylls remained fixed. Again, for both PSII and PSI the native arrangement of the conserved block of antenna chlorophylls was not optimal, even when considered within the complete antenna systems of PSII and PSI (data not shown; results very similar to Figures 2A and 2B). The orientations of the conserved antenna are thus not optimized for direct energy transfer to either RC or for facilitating energy transfer in the presence of the nonconserved chlorophylls unique to each photosystem.

Comparing the Efficiency of Other Photosynthetic Reaction Centers with Conserved Antenna

Recently it was discovered that the evolutionary conservation of residues that provide the axial ligand to the (bacterio)chlorophyll molecules is extended to photosynthetic complexes of green sulfur bacteria (*Chlorobium lumicola*) and heliobacteria (*Heliobacillus mobilis*) (Fyfe et al., 2002). Four His residues on each side of the photosystems are absolutely conserved between all four types of RCs. In PSII, two of these eight His are the ligands to the two $Chl_{Z/D}$ molecules. Our structural comparison of PSI and PSII shows that all eight chlorophylls coordinated by these conserved

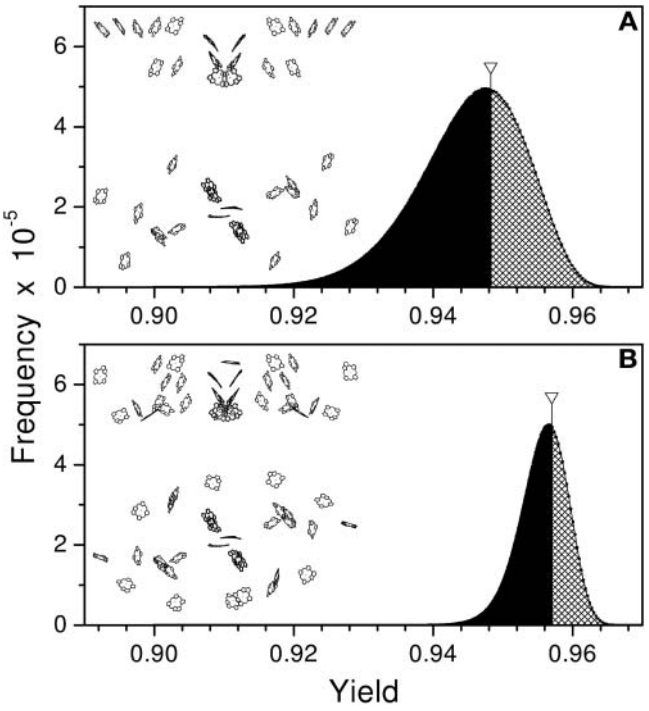

Figure 3. Histograms of the Quantum Yield Distributions Computed for Models of the Antenna Systems.

(A) Green sulfur bacteria *C. lumicola*.
(B) Heliobacteria *H. mobilis*.
The orientations of all antenna chlorophyll included in each model were varied. Inserts show the structure of the respective models. Arrows indicate the location of the quantum yield calculated with native chlorophyll orientations as found in the x-ray structures. Areas under the shadowed/black parts of the histograms represent the number of alternative pigment orientations with yields higher/lower than the native x-ray structure, respectively.

residues have virtually identical positions, macrocycles plane and dipole orientations. Models of the antenna domains of *C. lumicola* and *H. mobilis* RCs have been constructed previously, based on the x-ray crystal structure of PSI and sequence alignment data (Baymann et al., 2001; Fyfe et al., 2002). In that work all of the antenna (bacterio)chlorophyll in both *C. lumicola* and *H. mobili*s were assigned using analogs found within the larger PSI antenna structure. Are the conserved antenna subsystems of green sulfur bacteria and heliobacteria optimized for efficiency? Figure 3 shows distributions of the quantum yield computed for the hypothetical models of the antenna systems of *C. lumicola and H. mobilis*. In these simulations the orientations of all included antenna chlorophyll were randomized. It is clear that neither of these groups of conserved chlorophyll are optimal within these hypothetical ancestral structures.

In Search of Optimized Sites

None of the conserved chlorophyll arrangements we have investigated were found to be optimal for efficiency. However, as a whole, the entire antenna systems of PSI and PSII (with the exception of the $Chl_{Z/D}$ in PSII) are optimal. Clearly, the nonconserved chlorophyll must be responsible for the apparent optimality of the entire antenna system. Some of the nonconserved chlorophylls must make significant contributions to the variation in quantum yield and must also be highly optimized in their native orientations. Which chlorophylls are they?

To examine the optimality of each individual chlorophyll we changed its orientation in a model where all other antenna chlorophylls were fixed in their native orientations and calculated the resulting quantum yield for each orientation. We then determined the probability (*P*) of occurrence of orientations that resulted in a higher quantum yield than that calculated for the native orientation. Thus, the smaller the value of *P* the more highly optimized the native orientation of that individual chlorophyll. Simultaneously, we recorded the best and the worst quantum yields that resulted from all sampled orientations of each chlorophyll. The difference between the best and the worst quantum yield ($\Delta\phi$) represents a relative measure of the potential of each chlorophyll to affect the quantum yield.

Figure 4 shows plots of the dependence of $\Delta\phi$ on distance from the RC for each chlorophyll in PSII and PSI. As previously suggested for PSII (Vasil'ev et al., 2001), Figure 4A shows that the antenna chlorophyll closest to the reaction center, chlorophylls 31 and 14, have the highest impact on quantum yield. These two chlorophylls are ~20 to 22 Å away from the reaction center and

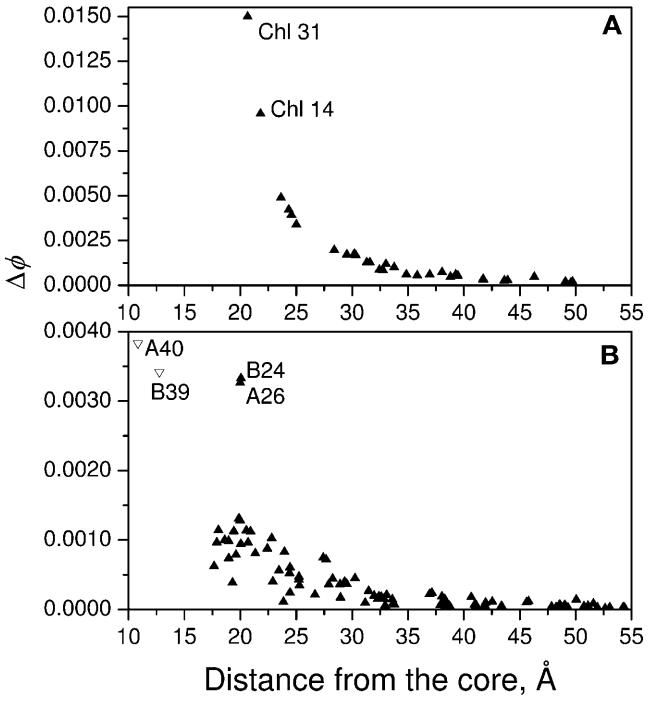

Figure 4. Dependence of the Difference ($\Delta\Phi$) between the Best and the Worst Quantum Yield Achieved by Reorientation of Individual Chlorophylls on Their Distance to the Closest Pigment in the RC Core.

(A) PSII.
(B) PSI.

only four additional chlorophylls are within 25 Å. As shown in Figure 4B the situation in PSI is quite different and more complex. There are four chlorophylls in PSI, previously identified as connecting chlorophylls (Sener et al., 2002), whose orientations have much more impact on quantum yield than any of the other chlorophylls. Two of them (chlorophylls A40 and B39) are only 10 to 12 Å from the reaction center chromophores whereas the other two (A26 and B24) are 20 Å distant. Interestingly, although there are 12 other chlorophylls physically closer to the RC than A26 and B24, and another 12 chlorophylls within 25 Å of the reaction center, they all have much lower potential to affect the quantum yield. The high impact of A26 and B24 on quantum yield in PSI arises from their strategic location, which allows them to act as bridging chlorophyll for a large number of other antenna chlorophylls. This makes them similar in function to chlorophylls 31 and 14 in PSII.

Figure 5 shows the dependence of P, the measure of orientational optimality, on $\Delta\phi$ for each chlorophyll in PSII and PSI. In PSII, chlorophylls 31 and 14 have the largest impact on quantum yield and are both found to be oriented optimally (Figure 6A). These two chlorophylls are the closest to the reaction center and do not have structural analogs in PSI. About half of the remaining chlorophylls show some degree of optimization whereas the other half do not, as expected for a random aggregate.

In PSI, the four chlorophylls that have the most impact on quantum yield show very different degrees of orientational optimization (Figure 5B). Chlorophylls A40 and B39 are not optimized whereas A26 and B24 are. None of these four chlorophylls have structural analogs in PSII, however, chlorophylls A26 and B24 in PSI appear to be functional analogs to chlorophylls 31 and 14 in PSII. Chlorophylls A40 and B39 are actually closer to the reaction center chromophores than they are to the antenna (Figure 4B) and may thus serve more than a light-harvesting role in PSI. Figure 5B shows no clear trend in the optimality of the less-potent antenna chlorophylls. About half of the remaining chlorophylls are optimized to some degree; the other half are not. This is true for antenna that do have structural analogs in PSII as well as for those that are unique to PSI.

Even though the overall structure of the antenna system in PSII is different from PSI, some similar features are seen in the arrangement of optimized chlorophylls (Figures 4A and 5A). In PSII, two bridging antenna chlorophylls, chlorophyll 14 and chlorophyll 31, have the largest potential to affect the quantum yield, are unique to PSII, and are highly optimized. In PSI chlorophylls A26 and B24 also have a large potential to affect quantum yield, are unique to PSI, and are highly orientationally optimized.

We conclude that both PSI and PSII antenna systems appear optimized as a whole only because of one pair of highly optimized bridging chlorophylls. To support this conclusion we calculated the distributions for the entire PSI and PSII antenna ensemble in which the orientations of all chlorophylls except the two optimized bridging chlorophylls were varied. These distributions are shown in Figure 6. It is clear that the orientations of the bulk chlorophylls in both PSI and PSII are not optimal. Interestingly, the pair of optimized chlorophylls is not conserved but is unique to each photosystem.

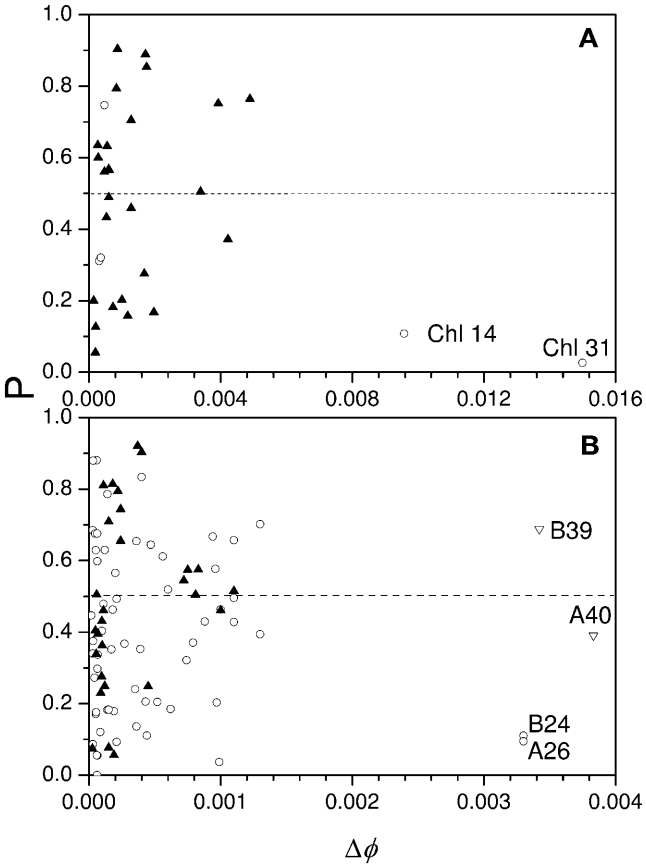

Figure 5. Plots of a Measure of Orientational Optimality (P) versus a Measure of the Potential of the Orientation of Each Individual Chlorophyll to Affect Quantum Yield ($\Delta\Phi$) in PSII and PSI.

P is the probability of occurrence of orientations that result in a higher quantum yield than that calculated for the native orientation. Thus, the smaller the value of P the more highly optimized the native orientation. In both **(A)** and **(B)**, solid upright triangles represent the 26 chlorophylls conserved between PSII and PSI and open circles the chlorophylls unique to each photosystem.

DISCUSSION

Beyond Orientation: The Effects of Spectral Composition

In this article we have studied the orientational optimality of light harvesting. There are alternative ways to optimize energy transfer between antenna pigments. Changing the energy levels of antenna pigments to change the spectral overlap between the emission spectrum of the energy donor and the absorption spectrum of the energy acceptor will affect efficiency and directionality of energy transfer. The spectral characteristics of antenna chlorophyll are modified by both pigment-protein and pigment-pigment interactions. Unfortunately, it is not yet possible to determine if spectral overlap is optimal because there is very little experimental data on the actual distribution of spectral forms within the core antenna of PSI and PSII.

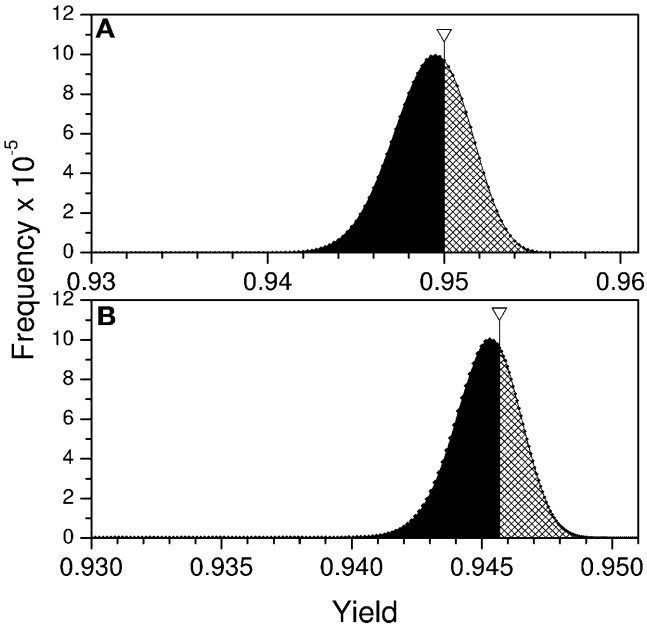

Figure 6. Histograms of the Quantum Yield Distributions Computed for the Complete Antenna Systems.

(A) PSII.

(B) PSI.

In the PSII model the orientations of all antenna chlorophylls except the two highly optimized chlorophylls (C14 and C31) and the two $Chl_{Z/D}$ were varied. In the PSI model the orientations of all antenna chlorophylls except the two highly optimized chlorophylls (B24 and A26) and chlorophylls A39 and B40 were varied. Inserts show the structure of the respective models. Arrows indicate the location of the quantum yield calculated with native chlorophyll orientations as found in the x-ray structures. Areas under the shadowed/black parts of the histograms represent the number of alternative pigment orientations with yields higher/lower than the native x-ray structure, respectively.

To determine whether the basic conclusions of our study are affected by spectral changes, we have tested the effects of energy level on the optimality of the two most important bridging chlorophylls in PSII and PSI by assigning their energy levels higher and lower than the rest of the antenna system. In PSII the energy levels of these two chlorophylls (C14 and C31) were adjusted by ± 220 cm^{-1}. This energy difference exceeds the limits predicted for the strongest possible coupling for either of these two chlorophylls with their nearest neighbor pigment (177 cm^{-1}). We have found that placing the energy level of C31 higher decreased its degree of optimization from 0.026 to 0.044, whereas placing its energy level lower increased optimality to 0.008. Similar results were obtained for C14. In all cases these pigments remained highly optimized. In PSI the maximal possible coupling of A26 and B24 to their closest neighbors is stronger than in PSII (620 cm^{-1}). Analogous to the situation in PSII, both A26 and B24 remained optimized when their energy levels were changed by ± 620 cm^{-1}. Furthermore, placing the energy levels of these pigments lower than the rest of the antenna system significantly increased their potential to affect quantum yield. Previous results from theoretical calculations performed with the PSI structure have suggested that these pigments are red-shifted (Damjanovic et al., 2002). Thus, there is evidence that the bridging chlorophylls, A26 and B24, may be even more important than predicted from our isoenergetic model.

Selection Pressures Affecting Core Antenna Structure

The quantum yield calculated from our models is directly related to the yield of stable charge separation in photosynthesis. The changes in quantum yield that are achieved by changing pigment orientations are small (a few percent) compared with the average quantum yield of PSI and PSII (usually >90%). This shows that relative core antenna pigment orientation has a fairly small effect on overall photosynthetic efficiency. Nevertheless, in both PSII and PSI, the orientations of specific core chlorophyll are highly optimized, indicating that such small changes in yield are sufficient for natural selection.

The optimization of quantum yield is important predominantly under light-limiting conditions, when light absorption falls short of metabolic demand. Under these conditions any small increase in quantum yield would be directly translated as more usable energy to the organism, and in the absence of strong competing selection pressures, could be selected for. Under conditions where light absorption exceeds metabolic demand, other reactions that compete for the deactivation of excited chlorophyll molecules and protect the organism from photooxidative stress can be expected to be more critical factors in the evolution of antenna systems, particularly in oxygenic photosynthesis. For example, the quenching of reactive species by carotenoids is a major photoprotective mechanism that may serve as a competing selection pressure for the relative positions and orientation of both core antenna chlorophyll and carotenoid molecules. Other selection pressures that could potentially affect the orientation of core antenna chlorophyll include, the facilitation of energy transfer between reaction centers, the coupling of a variety of peripheral antenna (including both bilin and chlorophyll binding polypeptides) to the core antenna, and the effectiveness of energy-regulating mechanisms like state transitions and/or high-energy quenching.

The core antenna of PSII and PSI face differing selection pressures. In the first instance, the two photosystems have very different strategies in core antenna organization, with the conserved block making up the majority of the core antenna in PSII but a much smaller part of the large ring of core antenna in PSI. The core antenna must also facilitate energy transfer between different peripheral antenna complexes in PSII and PSI. In addition, the two photosystems have different sensitivities to photooxidative damage and different regulatory and photoprotective strategies. Despite these differences the positions and orientations of the chlorophylls within the conserved block of pigments have remained remarkably unchanged during the independent evolution of PSII and PSI. What is the driving force for the conservation of the arrangement of this group of antenna pigments?

Structural considerations related to assembly and stability of the photosystems are a strong possibility. Clearly there are structural constraints that will limit the possible associations of porphyrins, especially the macrocycle, with the conserved

system of transmembrane α-helixes that make up all reaction centers. It is conceivable that a fairly limited number of positions and orientations are possible without drastically affecting assembly, stability, and/or the number of chlorophylls that can be held by the folding motif of these transmembrane α-helices. In light of the relatively small effect on quantum yield that relative orientation has for most antenna chlorophylls, it would not be surprising if structural considerations were a more important factor than energy-transfer efficiency for many of them. This is apparently the case for the conserved antenna chlorophylls.

Further work to understand the origin of this conservation will clearly require consideration of structural factors including the role played by the porphyrins in stabilizing the six membrane-spanning α-helix structural motif representative of the core antenna binding regions of PSII and PSI. In addition, a more detailed future study of optimization may show that more of the conserved chlorophylls are orientationally optimized within a smaller orientational search space that is limited by steric interactions between the chlorophylls and the existing protein structure. The conservation of the six-helix antenna chlorophyll binding protein motif exhibited by CP43 and CP47 and by the N-terminal region of PsaA and PsaB extends to the auxiliary CP43-like IsiA proteins of cyanobacteria and Pcb proteins of prochlorophytes containing chlorophyll *a* and chlorophyll *b*. These proteins serve to increase the antenna size of both PSI (CP43-like IsiA proteins under low iron levels in cyanobacteria, Bibby et al., 2001a; Pcb proteins under low light levels in Prochlorococcus, Bibby et al., 2001b) and PSII (Pcb proteins in Prochloron; Bibby et al., 2003). This structurally conserved six-helix chlorophyll binding motif has thus been used successfully in photosynthetic organisms as both core and peripheral antenna.

We have shown that both photosystems have a unique pair of antenna chlorophylls close to the RC whose orientations affect quantum yield more than any other antenna chlorophylls and whose native orientations are found to be optimal for bridging energy transfer to the RC. Their presence may reflect a combination of increased selection pressure on these strategically located chlorophyll and some level of increased structural freedom in the area between the five-member α-helical region of the reaction center and the six-member α-helical region of the core antenna binding region. In any case, unique solutions to the placement of key bridging chlorophylls appear to have arisen independently in PSII and PSI. Our results lead us to believe that optimized bridging chlorophylls may be a common feature of core light harvesting in photosynthetic RCs. We therefore predict that such optimized (bacterio)chlorophyll will be found to complement the conserved blocks of antenna (bacterio)chlorophyll already believed to exist in RCs of green sulfur bacteria and heliobacteria.

METHODS

Kinetic models for excited-state dynamics were constructed based on the x-ray structures of PSI and PSII from *Thermosynechococcus elongatus* (Jordan et al., 2001; Ferreira et al., 2004; Vasil'ev et al., 2004) and PSII from *Thermosynechococcus vulcanus* (Kamiya and Shen, 2003; Vasil'ev et al., 2004). The excitation transfer rates between chlorophylls were calculated based on Förster theory as described previously (Vasil'ev et al., 2002). The RC chlorophyll dimers P700 and P680 were represented as excitons with the lower excitonic states carrying most of the oscillator strength. The site energies of P700 and P680 were chosen to be 14,245 (Gillie et al., 1987) and 14,630 cm^{-1} (Smith et al., 2002), correspondingly. The site energies for the remaining chlorophylls were set at 675 nm (14,814 cm^{-1}). The master equation, describing time evolution of excitation in the system along with all chlorophyll sites, contained two additional sites representing primary electron acceptor (A_0 in PSI and Pheo in PSII) and secondary quinone electron acceptor (A_1 in PSI and Q_A in PSII). The yield of stable charge separation was calculated numerically as $\rho_{QA}(t)/\sum_i \rho_i(0)$, where ρ_{QA} denotes the probability that the quinone acceptor is reduced and $\sum_i \rho_i(0)$ is the total amount of excitation at time zero. Unimolecular decay rates were 0.5 ns^{-1}, the index of refraction was 1.5 (Gruszecki et al., 1999), the rate of charge separation was 1000 ns^{-1} (Gobets et al., 2003; Vasil'ev et al., 2003), and the rate of recombination 4.5 ns^{-1} for PSII and 0 ns^{-1} for PSI. In most of the simulations in our study we have chosen to neglect the spectral composition of the antenna by making all pigments isoenergetic. Although this approach facilitates the isolation of the orientational factor from other variables, we do not expect the absolute values of the quantum yields calculated from our models to reproduce the actual experimental values with high accuracy. To generate an ensemble of models with alternate arrangements of the transition dipoles we first generated the set of unit vectors by uniformly distributing 4096 points on a sphere of unit radius using the spiral algorithm (Saff and Kuijlaars, 1997). The ensemble is then formed by random independent selection of the dipole orientations from the set of unit vectors. Figures were produced with visual molecular dynamics (Humphrey et al., 1996).

ACKNOWLEDGMENTS

The authors gratefully acknowledge the support of Discovery and Equipment grants from the Natural Science and Engineering Research Council of Canada.

Received May 11, 2004; accepted August 26, 2004.

REFERENCES

Barber, J., and Andersson, B. (1994). Revealing the blueprint of photosynthesis. Nature **370,** 31–34.

Baymann, D., Brugna, M., Muhlenhoff, U., and Nitschke, W. (2001). Daddy, where did (PS)I come from? Biochim. Biophys. Acta. **1507,** 291–310.

Ben Shem, A., Frolow, F., and Nelson, N. (2003). Crystal structure of plant photosystem I. Nature **426,** 630–635.

Bibby, T.S., Nield, J., and Barber, J. (2001a). Iron deficiency induces the formation of an antenna ring around trimeric photosystem I in cyanobacteria. Nature **412,** 743–745.

Bibby, T.S., Nield, J., Chen, M., Larkum, A.W.D., and Barber, J. (2003). Structure of a photosystem II supercomplex isolated from *Prochloron didemni* retaining its chlorophyll a/b light-harvesting system. Proc. Natl. Acad. Sci. USA **100,** 9050–9054.

Bibby, T.S., Nield, J., Partensky, F., and Barber, J. (2001b). Oxyphotobacteria. Antenna ring around photosystem I. Nature **413,** 590.

Blankenship, R.E. (1992). Origin and early evolution of photosynthesis. Photosynth. Res. **33,** 91–111.

Byrdin, M., Jordan, P., Krauss, N., Fromme, P., Stehlik, D., and Schlodder, E. (2002). Light harvesting in photosystem I: Modeling based on the 2.5-angstrom structure of photosystem I from *Synechococcus elongatus*. Biophys. J. **83,** 433–457.

Damjanovic, A., Vaswani, H.M., Fleming, G.R., and Fromme, P. (2002). Chlorophyll excitations in photosystem I as revealed by semi-empirical ZINDO/CIS calculations. Biophys. J. **82,** 293 (abstr.).

Depaula, J.C., Innes, J.B., and Brudvig, G.W. (1985). Electron-transfer in photosystem-II at cryogenic temperatures. Biochemistry **24,** 8114–8120.

Faller, P., Rutherford, A.W., and Un, S. (2000). High-field EPR study of carotenoid(.+) and the angular orientation of chlorophyll z(.+) in photosystem II. J. Phys. Chem. B. **104,** 10960–10963.

Ferreira, K.N., Iverson, T.M., Maghlaoui, K., Barber, J., and Iwata, S. (2004). Architecture of the photosynthetic oxygen-evolving center. Science **303,** 1831–1838.

Fyfe, P.K., Jones, M.R., and Heathcote, P. (2002). Insights into the evolution of the antenna domains of type-I and type-II photosynthetic reaction centres through homology modelling. FEBS Lett. **530,** 117–123.

Gillie, J.K., Fearey, B.L., Hayes, J.M., Small, G.J., and Goldbeck, J.H. (1987). Persistent hole burning of the primary donor state of photosystem I: Strong linear electron-phonon coupling. Chem. Phys. Lett. **134,** 316–322.

Gobets, B., van Stokkum, I.H.M., van Mourik, F., Dekker, J.P., and van Grondelle, R. (2003). Excitation wavelength dependence of the fluorescence kinetics in photosystem I particles from *Synechocystis* PCC 6803 and *Synechococcus elongatus*. Biophys. J. **85,** 3883–3898.

Gruszecki, W.I., Grudzinski, W., Banaszek-Glos, A., Matula, M., Kernen, P., Krupa, Z., and Sielewiesiuk, J. (1999). Xanthophyll pigments in light-harvesting complex II in monomolecular layers: localisation, energy transfer and orientation. Biochim. Biophys. Acta. **1412,** 173–183.

Humphrey, W., Dalke, A., and Schulten, K. (1996). VMD: Visual molecular dynamics. J. Mol. Graph. **14,** 33–38.

Jordan, P., Fromme, P., Witt, H.-T., Klukas, O., Saenger, W., and Krauß, N. (2001). Three-dimensional structure of cyanobacterial photosystem I at 2.5 Å resolution. Nature **411,** 909–917.

Kamiya, N., and Shen, J.-R. (2003). Crystal structure of oxygen-evolving photosystem II from *Thermosynechococcus vulcanus at* 3.7-Å resolution. Proc. Natl. Acad. Sci. USA **100,** 98–103.

Klukas, O., Schubert, W.-D., Jordan, P., Krauß, N., Fromme, P., Witt, H.-T., and Saenger, W. (1999). Photosytem I, an improved model of the stromal subunits PsaC, PsaD, and PsaE. J. Biol. Chem. **274,** 7351–7360.

Krauß, N., Schubert, W.-D., Klukas, O., Fromme, P., Witt, H.-T., and Saenger, W. (1996). Photosystem I at 4 Å resolution represents the first structural model of a joint photosynthetic reaction centre and core antenna system. Nat. Struct. Biol. **3,** 965–973.

Michel, H., and Deisenhofer, J. (1988). Relevance of the photosynthetic reaction center from purple bacteria to the structure of photosystem II. Biochemistry **27,** 1–7.

Nitschke, W., and Rutherford, A.W. (1991). Photosynthetic reaction centers: Variations on a common structural theme. Trends Biochem. Sci. **16,** 241–245.

Rhee, K.H., Morris, E.P., Barber, J., and Kuhlbrandt, W. (1998). Three-dimensional structure of the plant photosystem II reaction centre at 8 Å resolution. Nature **396,** 283–286.

Saff, E., and Kuijlaars, A. (1997). Distributing many points on a sphere. Math. Intell. **19,** 5–11.

Schubert, W.-D., Klukas, O., Saenger, W., Witt, H.-T., Fromme, P., and Krauß, N. (1998). A common ancestor for oxygenic and anoxygenic photosynthetic systems: A comparison based on the structural model pf photosystem I. J. Mol. Biol. **280,** 297–314.

Sener, M.K., Lu, D.Y., Ritz, T., Park, S., Fromme, P., and Schulten, K. (2002). Robustness and optimality of light harvesting in cyanobacterial photosystem I. J. Phys. Chem. B. **106,** 7948–7960.

Smith, P.J., Peterson, S., Masters, V.M., Wydrzynski, T., Styring, S., Krausz, E., and Pace, R.J. (2002). Magneto-optical measurements of the pigments in fully active photosystem II core complexes from plants. Biochemistry **41,** 1981–1989.

Vasil'ev, S., Brudvig, G.W., and Bruce, D. (2003). The X-ray structure of photosystem II reveals a novel electron transport pathway between P680, cytochrome b(559) and the energy-quenching cation, Chl(Z)(+). FEBS Lett. **543,** 159–163.

Vasil'ev, S., Lee, C.-I., Brudvig, G.W., and Bruce, D. (2002). Structure-base kinetic modeling of excited-state transfer and trapping in His-tagged PSII core complexes from *Synechocystis*. Biochemistry **40,** 12236–12243.

Vasil'ev, S., Orth, P., Zouni, A., Owens, T.G., and Bruce, D. (2001). Excited-state dynamics in photosystem II: Insights from the x-ray crystal structure. Proc. Natl. Acad. Sci. USA **98,** 8602–8607.

Vasil'ev, S., Shen, J.-R., Kamiya, N., and Bruce, D. (2004). The orientations of core antenna chlorophylls in photosystem II are optimized to maximize the quantum yield of photosynthesis. FEBS Lett. **561,** 111–116.